Proc. R. Soc. Lond. B **218**, 455–477
Printed in Great Britain

A theoretical analysis of electrical properties of spines

By C. Koch[1]† and T. Poggio[2]

[1] *Max-Planck-Institut für biologische Kybernetik, Spemannstrasse* 38, *D*7400 *Tübingen, F.R.G.*

[2] *Department of Psychology and Artificial Intelligence Laboratory, Massachusetts Institute of Technology, Cambridge, Massachusetts* 02139, *U.S.A.*

(*Communicated by B. B. Boycott, F.R.S. – Received* 1 *March* 1983)

The electrical properties of a cortical (spiny) pyramidal cell were analysed on the basis of passive cable theory from measurements made on histological material (C. Koch, T. Poggio & V. Torre, *Phil. Trans. R. Soc. Lond.* B **298**, 227–264 (1982)).The basis of this analysis is the solution of the cable equation for an arbitrary branched dendritic tree. The conclusions, however, hold within a wide range of values of electrical parameters, provided that the membrane is passive. We determined the potential at the soma as a function of the synaptic input (transient conductance changes) and as a function of the spine neck dimensions, following a suggestion by W. Rall (*Brain Inf. Serv. Res. Rep.* **3**, 13–21 (1974); *Studies in neurophysiology* (ed. R. Porter), pp. 203–209 (Cambridge University Press, 1978)) that the spine neck might be an important determinant in regulating the efficiency of synapses on spines. From our investigation four major points emerge.

(i) Spines may effectively compress the effect of each single excitatory synapse on the soma, mapping a wide range of inputs onto a limited range of outputs (nonlinear saturation). This is also true for very fast transient inputs, in sharp contrast with the case of a synapse on a dendrite.

(ii) The somatic depolarization due to an excitatory synapse on a spine is a very sensitive function of the spine neck length and diameter. Thus the spine can effectively control the attenuation of its input via the dimensions of the neck, thereby setting the shape of the resulting saturation curve. There is an optimal neck diameter for which variations of the neck are most effective in controlling the weight of the excitatory spine synapse. For reasonable parameter values this optimal value is consistent with anatomical data. This might be the basic mechanism underlying ultra-short memory, long-term potentiation in the hippocampus or learning in the cerebellum.

(iii) Spines with shunting inhibitory synapses on them are ineffective in reducing the somatic depolarization due to excitatory inputs on the dendritic shaft or on other spines. Thus isolated inhibitory synapses on a spine are not expected to occur.

(iv) The conjunction of an excitatory synapse with a shunting inhibitory synapse on the same spine may result in a time-discrimination circuit with a temporal resolution of around 100 μs.

† Present address: Department of Psychology and Artificial Intelligence Laboratory, Massachusetts Institute of Technology, NE43–352, 545 Technology Square, Cambridge, Massachusetts 02139, U.S.A.

1. Introduction

Dendritic spines, first described by Cajal in Golgi preparation, were confirmed to be postsynaptic targets for a major portion of the synaptic inputs to pyramidal cells of the cortex (Gray 1959). Their functional role has remained a matter of speculation. Most of the early hypotheses considered the establishment of physical contact with presynaptic terminals as the main function of spines (for a modern view of this, see Swindale (1981)). More recently, however, dendritic spines have received increased attention as possible sites of neuronal plasticity.

A well studied case is the long-term potentiation (l.t.p.), an increase in the magnitude of either the intracellular excitatory postsynaptic potential (e.p.s.p.) or population spike, following tetanic stimulation of afferents in the hippocampal formation and lasting up to weeks (for a very thorough coverage of l.t.p. see Swanson *et al.* (1982)). Bliss & Lømo (1973) suggested as a possible mechanism of l.t.p. a reduction in the resistance of the narrow stem by which spines are attached to the parent dendrite, following a remark by Chang (1952) that the electrical resistance of the neck could be an important determinant of the synaptic 'weight'. Fifkova, Van Harreveld and others showed in a series of studies (Fifkova & Anderson 1981; Van Harreveld & Fifkova 1975; Fifkova & Van Harreveld 1977) that stimulation of the perforant path induces a long-lasting increase in the area of the dendritic spines, which are the postsynaptic sites on the stimulated pathways in the distal third of the dentate molecular layer. These changes were reversible and disappeared after a couple of hours (Fifkova & Van Harreveld 1977). Specifically, it could be shown that the spine necks increase in width and decrease in length (Fifkova & Anderson 1981). By adding a compound such as anisomycin that blocks protein synthesis, the enlargement of spines can be successfully suppressed, suggesting that the changing spine dimensions are caused by increased protein synthesis, possibly as a result of the creation of additional membrane (Fifkova *et al.* 1982). The same type of l.t.p. occurs in the mossy fibres to the CA3 and in the Schaeffer collaterals to the CA1 pyramidal cells in the hippocampus. A possible explanation would be again the enlargement of the postsynaptic spines (Andersen *et al.* 1980; Eccles 1979).

One can also try to influence experimentally the spine density and/or dimensions. Valverde (1967), in one of the first deprivation studies, found that the mean number of spines in visual cortex of visually deprived animals is significantly reduced in comparison with normally reared mice. In a different kind of deprivation experiment, in which community-reared and socially isolated jewel fish were compared, Coss & Globus (1978) observed that the community-reared fish have more dendritic branches and spines and, furthermore, that these spines have thicker and shorter stems than the spines of their isolated colleagues. Purpura (1974) and Marin-Padilla (1974) found, in the cortex of mentally retarded children, a reduced spine density and a significantly larger population of abnormally long, thin spines, concomitant with the absence of short, thick spines. Purpura (1979) has even suggested that some of the progressive neurobehavioural deteriorations (amentia) may be due to the degeneration of these spines. Bradley & Horn (1979) have exposed freshly hatched chicks to visual stimuli and looked at cells in the hyperstriatum, known by electrophysiology to be sensitive to early visual

experience. They find that the electrophysiological change in these cells after visual experience goes hand in hand with a morphological change: the spines have increased in size when compared with spines of dark-raised chickens. While all of these studies were performed under abnormal conditions, a few reports describe the effect of natural stimuli on spine shape. Boycott, in his study (1982) of spines on the Purkinje cells in hibernating and awake ground squirrels, found in the hibernating animals spines with enlarged spine heads, possibly leading to a decreased spine input resistance and thus to an enhanced excitability of these neurons during winter sleep. Rausch & Scheich (1982), when comparing young birds with speech-trained older birds, found a reduction in spine density and a concomitant enlargement in spine size in the latter group. One of the rare spine studies in insects (Brandon & Coss 1982; see also Coss *et al.* 1980) shows that the honeybees' first orientation flight, lasting on the average no more than 5 min, can already reduce spine neck dimensions and increase spine head diameter, without lowering the overall spine length. All these observations strongly support an important role of spine plasticity under normal stimuli conditions.

If spines are modifiable, a study of their electrical properties becomes especially important. In contrast, however, with the numerous experimental findings, there have been only a few theoretical analyses of spines. Rall (1970, 1974, 1978; see also Jack *et al.* 1975) gave an estimate of the effect of a variable spine geometry on the somatic potential induced by an active synapse on the spine. He pointed out that to achieve maximal plasticity of spines, i.e. small variations of the spine neck diameter producing large variations in the somatic depolarization, there must be a kind of impedance matching between the spine neck and the dendrite, causing distal spines to be longer and thinner than proximal ones. Recently, Crick (1982) conjectured that dendritic spines are involved in some kind of ultra-fast memory, on the scale of seconds or even milliseconds. In this picture spines would be constantly changing their shape in response to the synaptic input.

In this paper we shall extend the results of Rall in a study of a real cortical pyramidal cell with transient conductance changes as inputs. We shall then discuss several non-exclusive hypotheses on the function of dendritic spines.

2. Methods

The main tool that we have used is a (PASCAL) program that computes the transfer function $\tilde{K}_{ij}(\omega)$ for current input at location i and voltage output at location j as a function of frequency ω in any given passive dendritic structure (Koch *et al.* 1982). The direct current (d.c.) value $K_{ij}(0)$ of the transfer function is the ohmic transfer resistance seen for steady-state current inputs ($V_j = \tilde{K}_{ij}(0)I_i$). If the two locations i and j coincide, one obtains the familiar input impedance at that location ($\tilde{K}_{ii}(\omega)$ is the impedance seen by an electrode for current injections). The complex functions $\tilde{K}_{ij}(\omega)$, for various locations i and j, completely characterize the (linear) electrical properties of a branched passive cable. Any given current input with a Fourier transform $\tilde{I}_i(\omega)$ at location i can be 'propagated' by the associated $\tilde{K}_{ij}(\omega)$ to another location j to give the resulting depolarization:

$$\tilde{V}_j(\omega) = \tilde{K}_{ij}(\omega)\,\tilde{I}_i(\omega). \tag{1}$$

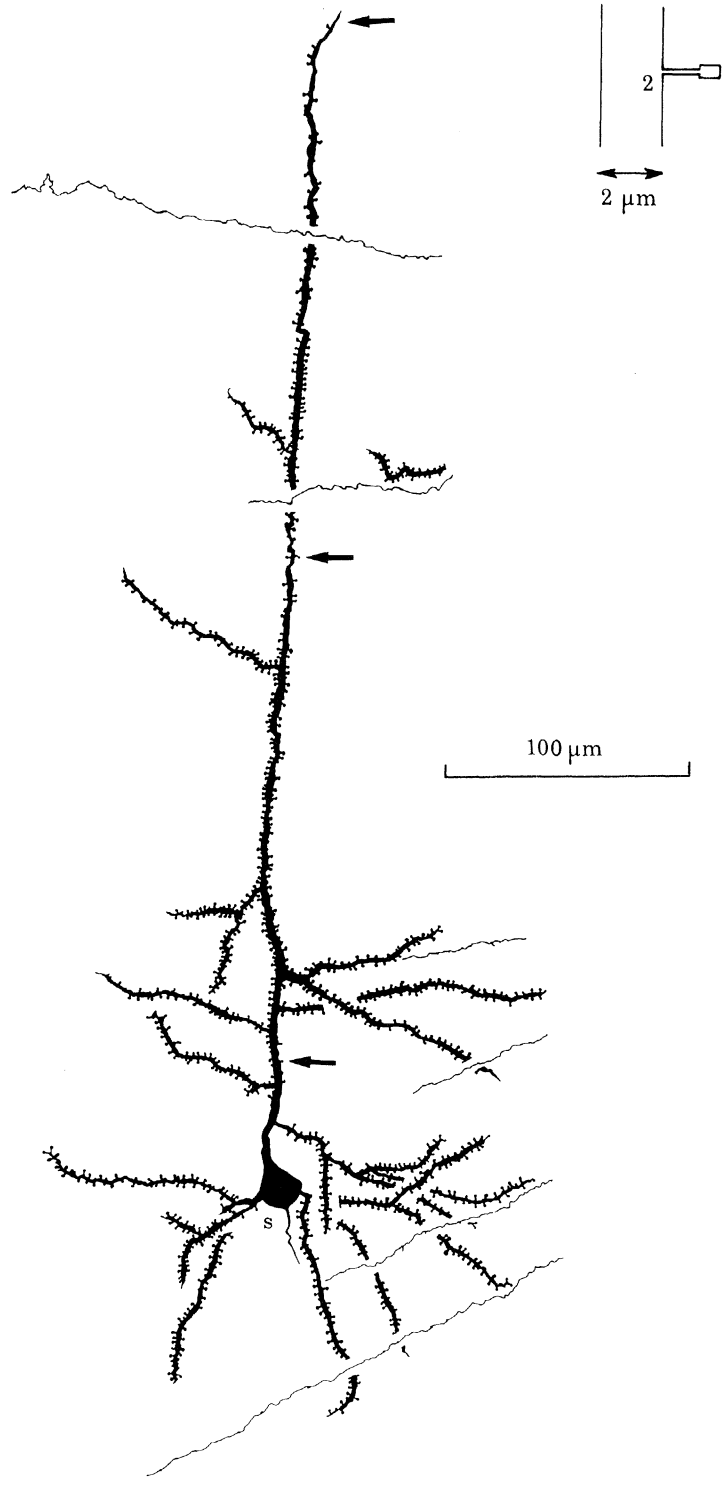

FIGURE 1. For description see opposite.

The algorithm implemented by the program is basically due to Butz & Cowan (1974; see also Koch 1982) and is based on classical one-dimensional cable theory (for a review see Jack *et al.* (1975) or Rall (1977)). The membrane is assumed to be passive. Instead of approximating the dendrite as a series of isopotential lumped compartments we describe a dendritic structure as a sequence of cylinders, where each branch (or part of a branch) is represented by a cylinder of appropriate length and diameter. This method does not place any restriction on the geometrical structure of the dendritic tree considered nor, unlike Rall's $d^{\frac{3}{2}}$ power law, on the diameters of the branches. The Green functions $K_{ij}(t)$, i.e. the inverse Fourier transforms of $\tilde{K}_{ij}(\omega)$, are then exact solutions (for delta pulses of current) of the cable equation for this model.

3. Our model of the pyramidal cell

We calculated the electrical properties of spines on the basis of measurements made on a Golgi-stained pyramidal cell (kindly provided by V. Braitenberg) from the sensory-motor cortex of an adult mouse. From this preparation (see figure 1) we determined the branching structure, the length and the diameters of each dendritic segment as described in detail elsewhere (Koch *et al.* 1982). If not otherwise stated, we used $R_m = 4000\ \Omega\ \mathrm{cm}^2$ for the membrane resistance, $R_i = 70\ \Omega$ cm for the intracellular resistance and $C_m = 2\ \mu\mathrm{F\ cm}^{-2}$ for the membrane capacity, resulting in a membrane time constant of 8 ms (Creutzfeldt *et al.* 1964). The reversal potential of the excitatory synapse, E_1, is always equal to 80 mV relative to the resting potential of the cell. We shall discuss the effect of different neuronal parameters on our results later.

The spines were modelled by a thin and narrow cylinder, called the spine neck and by a thick, short cylinder simulating the spine head (see inset in figure 1). Except when otherwise stated, the spine neck is 0.1 μm thick and 1.0 μm long and the head is 0.3 μm thick and 0.6 μm long (for the exact morphology of spines see Coss *et al.* (1980) or Westrum & Blackstad (1962)). In all cases considered further on, the total spine area is always constant and equal to 0.96 $\mu\mathrm{m}^2$. Because of limitations in storage space and computation time, we simulated the pyramidal cell (in figure 1) with only 10 spines, instead of the 1000 or more spines that are actually present. To test the effect of this approximation on our results, we compared the somatic depolarization due to an active synapse in a small cell with the usual spine density (*ca.* 1.7 spines per micrometre (Schüz 1976)) with the somatic potential in the same cell without any spines. Owing to the extremely small neck of the spines, practically no current enters the spines and the potential in the two cases differed by at most 1.5%.

Figure 1. The pyramidal cell used throughout our simulations from sensory-motor area of the mouse cortex. The fine horizontal lines are axons from other cells. Golgi preparation by V. Braitenberg. The electrotonic distance from the spine to the soma is 1.19, 0.59 and 0.08 length constants for the distal, middle and proximal spine respectively (for $R_m = 4000\ \Omega\ \mathrm{cm}^2$ and $R_i = 70\ \Omega$ cm). The inset shows our model of the spine. The arrows point to the spines whose properties are studied. Redrawn from Koch & Poggio (1983).

4. Linear electrical properties of spines

Let us first consider the electrical properties of the spine for current inputs. In this case the input–output relation between a current input $I_i(t)$ at i and the resulting voltage output $V_j(t)$ at j is linear, i.e.

$$V_j(t) = K_{ij}(t) * I_i(t) \tag{2a}$$

or, in the Fourier domain,

$$\tilde{V}_j(\omega) = \tilde{K}_{ij}(\omega)\,\tilde{I}_i(\omega), \tag{2b}$$

where $*$ represents the convolution operation. The d.c. resistance of the spine neck is given by

$$R_N = 4R_i\, l_N/\pi d_N^2. \tag{3}$$

R_N is the resistance of a cylinder with R_i being the specific resistance of the cytoplasm, d_N the spine neck diameter and l_N the spine neck length. We call $\tilde{K}_H(\omega)$ the impedance of the spine head and we model it as a very high membrane resistance $R_H = R_m/F_H$ in parallel with the capacitance $C_H = C_m F_H$ where F_H is the membrane area of the spine head. Thus

$$\tilde{K}_H(\omega) = R_H/(1+i\omega\tau_m) \tag{4}$$

where $\tau_m = R_m C_m$ is the time constant of the neuron. The current that is injected into the spine can either flow out through the membrane of the spine head with the impedance $\tilde{K}_H(\omega)$ or flow through the spine stem with the impedance R_N and onward into the dendritic shaft which has the input impedance $\tilde{K}_{22}(\omega)$ (we designate by 1 the location of the spine head and by 2 the location of the dendritic shaft just below the spine; see inset in figure 1). Neglecting the very small current losses through the membrane of the spine neck, we obtain the approximation (see also Rall 1978)

$$\frac{1}{\tilde{K}_{11}(\omega)} \approx \frac{1}{\tilde{K}_{22}(\omega)+R_N} + \frac{1}{\tilde{K}_H(\omega)}. \tag{5}$$

If we observe that, for our standard parameters, $\tilde{K}_H(\omega) \gg \tilde{K}_{22}(\omega)$ and $R_N/R_H \ll 1$, we arrive at

$$\tilde{K}_{11}(\omega) = (\tilde{K}_{22}(\omega)+R_N)/(1+i\omega\tau_s) \tag{6}$$

where $\tau_s = R_N C_H$ is the time constant of the spine. Thus the spine input impedance equals the dendritic shaft input resistance plus the spine neck resistance filtered by the low-pass spine filter function $1/(1+i\omega\tau_s)$, where the spine time constant τ_s depends only on spine geometry. For our standard values of spine neck dimensions we find $R_N = 87.25$ MΩ, $\tau_s = 0.98$ μs and $\tau_m = 8.00$ ms (for a detailed derivation of these results see Koch (1982)).†

If we consider now the transfer impedance $\tilde{K}_{12}(\omega)$ from the spine head to the base of the spine, we find that $\tilde{K}_{12}(\omega)$ is the product of the dendritic input impedance and the spine filter function i.e.

$$\tilde{K}_{12}(\omega) = \tilde{K}_{22}(\omega)/(1+i\omega\tau_s) \tag{7}$$

† We compared the computed (exact) value of $\tilde{K}_{11}(\omega)$ with $\tilde{K}_{11}(\omega)$ determined with the approximation equation (6), $\tilde{K}_{22}(\omega)$ being also calculated with the help of our program. These two functions differ by (at most) 3.1 %.

Since τ_s is very small (much smaller than the typical time constant of $\tilde{K}_{12}(\omega)\tau_m$), for low frequencies essentially all the injected current reaches the dendritic trunk. Only at high frequencies (with respect to τ_s^{-1}) do losses take place because of the very small surface of the spine.

In the following we shall make use of two relations that hold for an arbitrary tree without loops (Koch 1982; Koch *et al.* 1982):

$$\tilde{K}_{ij}(\omega) = \tilde{K}_{ji}(\omega), \tag{8a}$$

$$\tilde{K}_{ij}(\omega) = \tilde{K}_{il}(\omega)\,\tilde{K}_{lj}(\omega)/\tilde{K}_{ll}(\omega), \tag{8b}$$

where l is any location on the direct path from location i to j. For the transfer function from spine head to soma we find therefore

$$\tilde{K}_{1s}(\omega) = \tilde{K}_{12}(\omega)\,\tilde{K}_{2s}(\omega)/\tilde{K}_{22}(\omega) = \tilde{K}_{2s}(\omega)/(1+i\omega\tau_s). \tag{9}$$

However, since $\tilde{K}_{2s}(\omega)$ drops rapidly to zero (in the order of τ_m^{-1} Hz) the spine filter function can be considered essentially flat over this range and therefore

$$\tilde{K}_{1s}(\omega) = \tilde{K}_{2s}(\omega). \tag{10}$$

(When $\tilde{K}_{1s}(\omega)$ is compared with $\tilde{K}_{2s}(\omega)$, equation (10) holds within 0.02 %.) Again this is due to the fact that practically all the injected current reaches the dendritic trunk. In other words, the depolarization due to a current input at some other location in the dendritic tree (for instance the soma) is the same, irrespectively of whether the synapse is on the spine or directly on the dendrite. In short, in the linear (current) case, spines do not isolate. By the same argument, spines are no more electrically isolated from a current input at an arbitrary location than synapses directly on the dendritic stem. Specifically, the depolarization induced by the antidromic invasion of a somatic spike, based on the assumption of a passive membrane, is the same on the dendritic trunk as in the spine head.

Notice that these results hold for the overall transfer function and therefore for any d.c. or transient current input. Thus, if synaptic inputs were described as current inputs (and the membrane is assumed passive), it would not matter whether synapses are on spines or directly on the dendritic trunk.

5. Synaptic inputs on spines are nonlinear

Synaptic inputs, however, consist of transient conductance changes to specific ions and are not currents. Synaptic inputs effectively open 'holes' in the membrane for ions with a reversal potential E_1 measured with respect to the local resting potential V_{rest}. If the conductance for a specific ion changes by the amount $g_1(t)$ and $V_1(t)$ is the membrane potential change at the synapse relative to the resting potential, we have the following expression for the current

$$I_1(t) = g_1(t)\,[E_1 - V_1(t)]. \tag{11}$$

The change in voltage is then given by a Volterra-integral equation

$$V_1(t) = K_{11}(t) * \{g_1(t)\,[E_1 - V_1(t)]\}. \tag{12}$$

Because spines have a high input impedance, even a small and very fast

conductance change may easily drive the local potential in the spine towards the equilibrium potential E_1, considerably reducing the amount of inflowing current and therefore the depolarization at the soma (or some other location).

5.1. *Steady-state inputs*

We shall first restrict ourselves to steady-state conductance changes g_1, while the more general case of transient inputs $g_1(t)$ will be regarded later on. In the steady-state case, equation (12) takes the form

$$V_1 = \tilde{K}_{11}(0)\, g_1(E_1 - V_1). \tag{13}$$

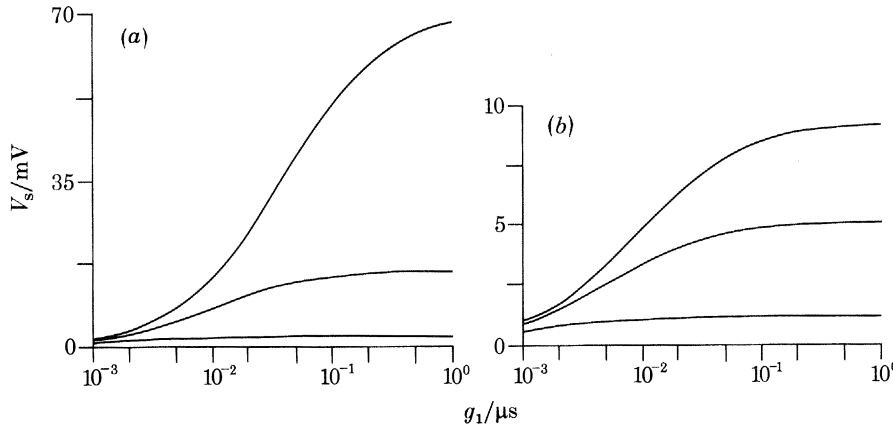

FIGURE 2. (*a*) Nonlinear saturation of the somatic voltage as a function of a steady-state conductance input g_1 for three different cases: the synapse lies on the dendritic shaft directly below a proximal spine (top curve); the synapse is situated on the spine head of a proximal spine with the standard neck dimensions ($d_N = 0.1$ μm and $l_N = 1.0$ μm; middle curve); and the synapse lies on the spine head of a proximal spine with a stretched spine neck ($d_N = 0.05$ μm and $l_N = 2.0$ μm; lower curve). (*b*) Same as (*a*), except that the distal spine of figure 1 has been used. (Notice the decrease in voltage scale.)

With the use of equation (2*a*), the depolarization V_s at the soma (relative to V_{rest}) is given by

$$V_s = g_1 K_{1s} E_1/(1 + g_1 K_{11}) \tag{14}$$

where K_{11} and K_{1s} are the steady-state impedances $\tilde{K}_{11}(0)$ and $\tilde{K}_{1s}(0)$. V_s can be rewritten as:

$$V_s = ASE_1, \tag{15}$$

where A is the attenuation factor $A = K_{1s}/K_{11}$ and S is the spine factor $S = g_1 K_{11}/(1 + g_1 K_{11})$. A, which is the voltage attenuation between the locations 1 and s, depends only on the neuronal geometry, while the spine factor S, reflecting the nonlinear addition at the spine (also called nonlinear saturation), is a function of the conductance input and the spine geometry; the potential change at the spine, due to a conductance change g is given by SE_1 (of course, both A and S depend on neuronal parameters such as R_m and R_i). Equation (14) represents a kind of gain control mechanism. For small inputs, V_s is essentially proportional to g_1 and for large inputs it saturates to $E_1\, K_{1s}/K_{11}$ (see figure 2).

Figure 2 shows the somatic potential as a function of the input g_1 for a proximal (figure 2*a*) and a distal spine (figure 2*b*). The top curve is the somatic potential V_s generated by a synapse on the dendritic shaft (this can be interpreted as the limiting case of a spine with $d_N \to \infty$ and $l_N \to 0$), the middle curve is the potential for our standard spine ($d_N = 0.1$ μm, $l_N = 1.0$ μm) and the bottom curve is the potential for a spine where the neck has been stretched ($d_N = 0.05$ μm, $l_N = 2.0$ μm).

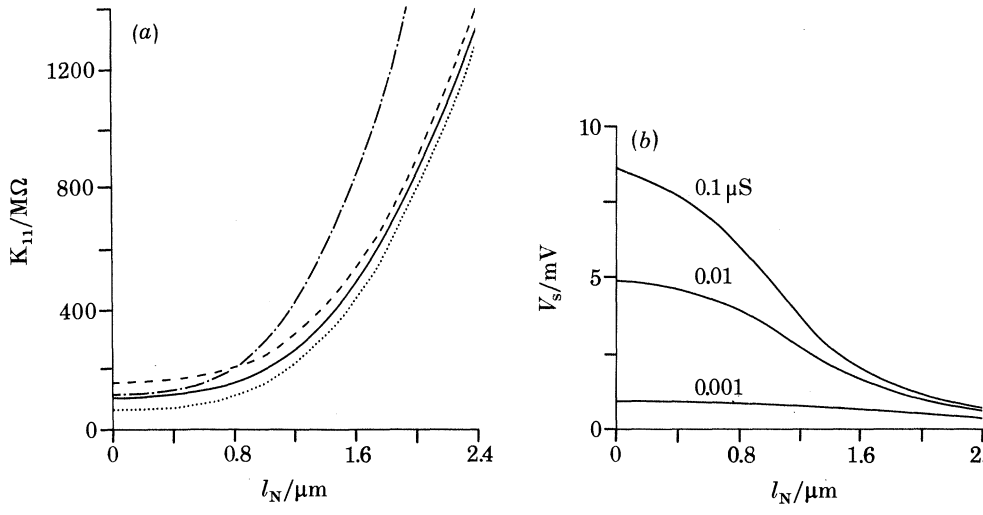

FIGURE 3. (*a*) The d.c. input impedance $\tilde{K}_{11}(0) = K_{11}$ (for the distal spine) as a function of the spine neck length and diameter calculated for different membrane parameters (the spine neck dimensions were changed in such a way as to leave the total neck surface area constant: $d_N l_N = 0.1$ μm^2). The solid curve is for $R_m = 4000$ Ω cm^2, the dotted curve is for $R_m = 1000$ Ω cm^2 and the dashed curve is for $R_m = 16000$ Ω cm^2; while for these curves R_i is everywhere homogeneous with $R_i = 70$ Ω cm; for the dot–dashed curve $R_m = 4000$ Ω cm^2 and $R_i = 70$ Ω cm holds in the soma and dendrites but R_i has twice this value (140 Ω cm) for the cytoplasm of the spine. The corresponding transfer resistances to the soma are 12.75, 1.51, 39.25 and 12.75 MΩ. (*b*) The somatic depolarization for the distal spine of figure 1 with changing spine neck dimensions (see (*a*)) for different inputs.

For steady-state inputs equation (6) can be used to determine the input resistance of a spine:

$$K_{11} = K_{22} + R_N = K_{22} + 4R_i l_N / \pi d_N^2. \tag{16}$$

Depending on the dimensions of the neck, R_N can be very much larger than K_{22}, implying that K_{11} depends strongly on the spine neck diameter and length. A relatively small change in d_N or l_N will then lead to a large change in K_{11} with corresponding changes in the somatic potential. Figure 3*a* demonstrates this effect. For a distal spine (see figure 1) we stretched or contracted the spine neck in such a way, as to leave the total neck surface area constant ($l_N d_N = 0.1$ μm^2). Thus increasing the neck length goes hand in hand with a decrease in neck diameter. Figure 3*b* shows the corresponding change in spine potential for different synaptic inputs.

5.2. *Transient inputs*

Until now we have only considered steady-state inputs g_1. It may be argued that our picture of the spine changes appreciably when transient conductance changes $g_1(t)$ are considered. With this kind of input, it is in general impossible to write the depolarization in a closed analytical form, although the solution of the Volterra equation can be determined by simple numerical integration.

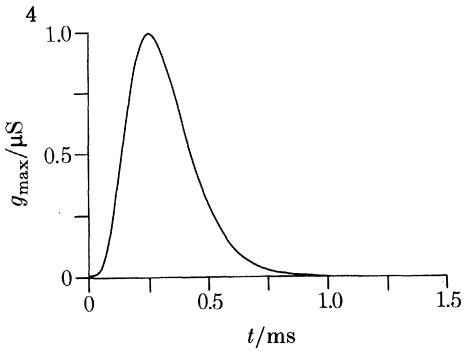

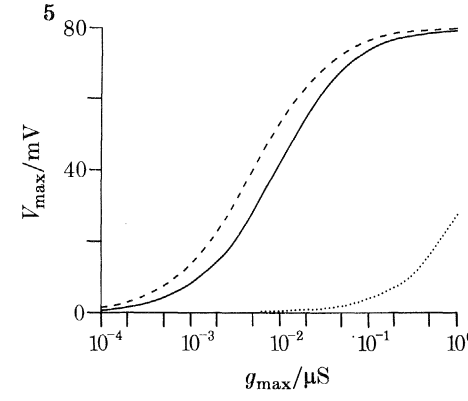

FIGURE 4. The time course of the conductance change $g_1(t) = g_{max}\, t_{peak}^{-4}\, e^4\, t^4\, e^{-4/t_{peak}}$ shown here with $t_{peak} = 0.25$ ms and $g_{max} = 1$. The pulse has decayed to zero after about 0.9 ms.

FIGURE 5. The maximum depolarization at the synapse, for a fast transient conductance input of peak amplitude g_{max} ($t_{peak} = 0.25$ ms and total duration 0.9 ms) at the distal spine of figure 1 (solid line) or at the dendritic shaft just below the spine (dotted line). The dashed line shows that a steady state conductance change yields essentially the same depolarization in the spine as the transient input; $\tau_m = 8$ ms.

Owing to the very small membrane area of a spine (the surface of our standard spine is approximately 1 μm²), the total spine capacity is exceedingly small, leading to large impedance values even at high frequencies. Thus a significant saturation and 'choking' effect would take place even for very fast transient inputs. We have demonstrated this effect using a fast conductance change $g_1(t)$ with a time-to-rise (t_{peak}) of 0.25 ms and a total duration of 0.9 ms (compare this with $\tau_m = 8$ ms). The time course of $g_1(t)$ is given by

$$g_1(t) = \text{const.} \times t^4\, e^{-4t/t_{peak}}$$

and is shown in figure 4.† Figure 5 shows the maximum of the depolarization at the synapse as a function of the amplitude of the maximal conductance change g_{max}. The solid curve shows the evoked potential at the spine head due to an active synapse at this spine, while the comparable steady state input change g_{max} yields the dashed curve similar to the transient curve. An active synapse at the dendritic shaft just below the spine gives rise to a much smaller depolarization, showing very little saturation. In contrast with the dendrite, the spine shows essentially the same saturation behaviour for fast as for slow inputs. This is an important point: relative

† The constant is equal to $g_{max}\, t_{peak}^{-4}\, e^4$, where g_{max} is the maximum value of $g(t)$ at $t = t_{peak}$.

saturation effects and peak voltage in a spine, compared with the dendrites, are much greater for transient inputs than for steady state inputs. Thus, transient conductance inputs maximize the difference between a synapse on a spine and a synapse on the dendritic shaft.

To compare the influence of the spine neck on transient inputs with our previous results on the steady-state change in somatic voltage, we defined a real number K_{ij}^{eff} expressing the resistance between the points i and j for a given transient input

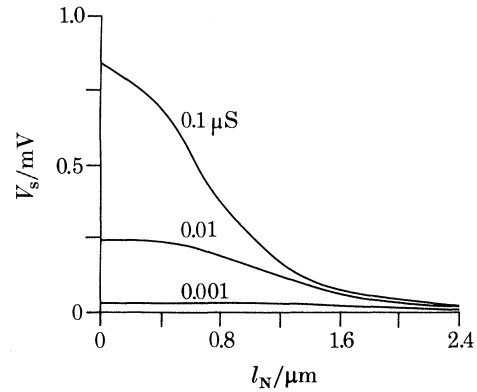

FIGURE 6. Somatic depolarization as a function of spine geometry and maximal amplitude of the transient conductance change for a distal spine. V_s was approximated by using K^{eff} for a conductance input with $t_{\text{peak}} = 0.25$ ms (see figure 3*b*).

(see Koch (1982) for a detailed derivation). Replacing $\tilde{K}_{11}(\omega)$ by K_{11}^{eff} and $\tilde{K}_{1s}(\omega)$ by K_{1s}^{eff} we can approximate the resulting somatic potential due to a transient conductance input $g_1(t)$ to a very satisfactory degree (the maximal depolarization at the spine head in figure 5 deviates at most by 1.3 % from the voltage determined via K^{eff}). The voltage approximation always lies below the solution of the full Volterra equation, thus giving a lower bound on the voltage generated by a transient synaptic input (for proof see Koch (1982)). Figure 6, corresponding to figure 3*b*, shows the dependence of peak somatic voltage for three fast transient inputs at different maximal amplitudes as a function of spine dimensions. Except for a difference in scale due to high-frequency losses through the membrane capacity, the basic conclusion is still valid: somatic depolarization depends strongly on spine dimensions.

6. WHAT IS THE OPTIMAL NECK DIAMETER?

If the 'weight' of the synapse is adjusted by small variations of the spine neck, it is relevant to ask under what conditions the smallest change in d_N and/or l_N results in the largest change in V_s. Under the assumption that the total membrane area ($d_N l_N$ = const.) is constant, this can be expressed formally by

$$\frac{\partial^2}{\partial l_N^2}\left(\frac{g_1 K_{1s}}{1+g_1 K_{11}}\right) = 0. \tag{17}$$

Equations (10) and (16) being taken into account, equation (17) gives

$$R_N = 1/2g_1 + \tfrac{1}{2}K_{22}. \tag{18}$$

Rall has pointed out (for the case of maximum saturation, i.e. $g_1 \to \infty$) that this kind of impedance matching between the spine neck and the dendritic shaft to which the spine is attached, implies a systematic variation of spine geometry with distance from the soma: because the soma is a current sink, K_{22} will decrease with decreasing distance to the soma and consequently so will the spine neck resistance R_N. Thus, depending on synaptic strength and on the position of the spine, spines should be shorter and thicker for proximal locations and longer and thinner for distal locations in order to maximize synaptic 'plasticity' (for the functional consequences see Discussion, §9.

7. Interactions between two synaptic inputs

Up to now we have only considered the effect of a single synaptic input on the potential. But what happens when two or more synapses are simultaneously active? One can distinguish two important cases: nonlinear interaction between inputs of different types, i.e. between an excitatory and an inhibitory synapse; and nonlinear addition between inputs of the same type.

7.1. *Nonlinear interaction*

Let us consider the case of an excitatory synapse at location e modulating the conductance change $g_e(t)$ of an ionic species with equilibrium potential $E_e > 0$ (relative to V_{rest}) and an inhibitory synapse modulating the conductance change $g_i(t)$ to an ionic species with equilibrium potential $E_i \leqslant 0$ at location i (the locations i and e can coincide). For transient conductance inputs the system of coupled Volterra integral equations giving the resulting change in somatic potential is:

$$\left.\begin{aligned} V_s(t) &= \{g_e(t)[E_e - V_e(t)]\} * K_{es}(t) - \{g_i(t)[E_i - V_i(t)]\} * K_{is}(t), \\ V_e(t) &= \{g_e(t)[E_e - V_e(t)]\} * K_{ee}(t) - \{g_i(t)[E_i - V_i(t)]\} * K_{ie}(t), \\ V_i(t) &= \{g_e(t)[E_e - V_e(t)]\} * K_{ei}(t) - \{g_i(t)[E_i - V_i(t)]\} * K_{ii}(t). \end{aligned}\right\} \tag{19}$$

To maximize the nonlinear interaction between these two different inputs, we shall consider only shunting inhibition, i.e. $E_i = 0$ (relative to the resting potential). A simple measure of the effectiveness of shunting inhibition is the ratio (called F-factor) between the maximum somatic depolarization in the absence of inhibition to the maximum of the somatic depolarization in the presence of the inhibitory input.

In the case of steady-state inputs, the F-factor is given by (see Koch *et al.* 1982)

$$F_{dc} = \frac{g_e K_{es}}{1 + g_e K_{ee}} \frac{1 + g_e K_{ee} + g_i K_{ii} + g_i g_i (K_{ee} K_{ii} - K_{ei}^2)}{g_e K_{es} + g_e g_i (K_{es} K_{ii} - K_{ei} K_{is})} \tag{20}$$

Table 1 shows F_{dc} for four typical situations: both synapses are on the spine, both synapses are on the dendritic shaft and one synapse is on the spine while the opposing synapse lies on the dendrite.

Two conclusions can be drawn from these and similar results.

(i) An inhibitory synapse situated alone on a spine is usually ineffective in reducing the potential at some other location. This is in accordance with the general on-the-path property (Koch *et al.* 1982): inhibition is most effective when it is located on the direct path between excitation and soma.

(ii) If the excitatory synapse lies on the spine, it does not make much difference whether the inhibition is directly adjacent or on the dendrite (between the spine and the soma).

TABLE 1. F VALUES FOR STEADY-STATE INPUTS IN THE PYRAMIDAL CELL OF FIGURE 1

(Both the excitation e ($E_e = 80$ mV) and the shunting inhibition i ($E_i = 0$ mV) are located exactly below or on the spine in the middle portion of the apical tree. The depolarization at the soma due to excitation on the spine (on the dendrite just below the spine) without inhibition is 1.06 mV (1.15 mV) for $g_e = 0.001$ μS, 4.99 mV (7.87 mV) for $g_e = 0.01$ μS and 7.95 mV (19.04 mV) for $g_e = 0.1$ μS.)

$g_e/\mu S$ ...	10^{-3}	10^{-2}	10^{-3}	10^{-2}	10^{-1}	10^{-3}	10^{-2}	10^{-1}	10^{-1}
$g_i/\mu S$ ...	10^{-3}	10^{-3}	10^{-2}	10^{-2}	10^{-2}	10^{-1}	10^{-1}	10^{-1}	10^{0}
				values of F					
e on spine, i on spine	1.12	1.06	2.24	1.59	1.01	13.41	6.86	1.93	10.34
e on spine, i on dendrite	1.05	1.04	1.51	1.42	1.35	6.09	5.16	4.46	3.56
e on dendrite, i on spine	1.05	1.03	1.27	1.18	1.04	1.51	1.35	1.09	1.09
e on dendrite, i on dendrite	1.05	1.03	1.51	1.35	1.08	6.07	4.48	1.84	9.42

Conclusion (i) implies that one would not expect to observe any inhibitory synapses on spines in histological preparations (see Discussion).

When transient inputs are considered, the relative timing between them is an important determinant for the degree of interaction (see Koch *et al.* 1983). We solved numerically the system of integral equations (19) for the case when both synapses are either on the spine or on the dendrite. As input functions we used fast transients with $t_{peak} = 0.25$ ms for both inputs (see figure 4). The shunting inhibition had a peak conductance value ($g_{i\,max}$) of 10^{-7} S, while the excitation was ten times weaker ($g_{e\,max} = 10^{-8}$ S), but the main properties of the interaction do not depend on it. Figure 7 shows the resulting 'tuning curve' of the F-factor. What is especially remarkable is that the vetoing effect of inhibition is very sharply dependent on relative timing between the two inputs. Whereas inhibition on the dendritic shaft can effectively veto excitation within a temporal window of the order of $\pm t_{peak}$, inhibition on a spine is stronger and more selective, being effective only in a window of $\pm \frac{1}{2} t_{peak}$ (± 120 μs around the start of excitation).

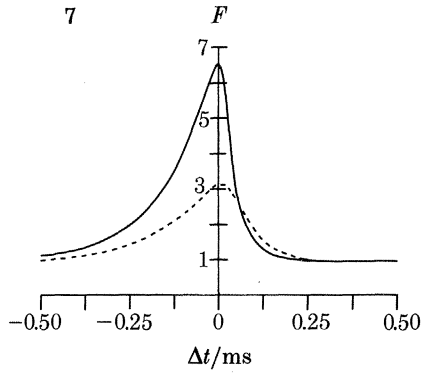

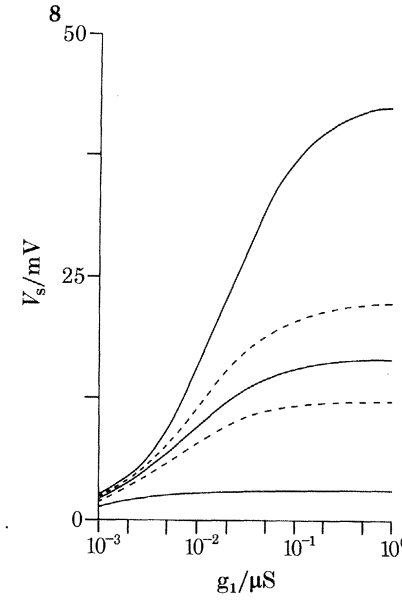

FIGURE 7. F-factor (ratio of the maximum of the somatic depolarization without inhibition to the somatic depolarization in the presence of inhibition) for synapses on the spine head of a distal spine (continuous curve) or on the dendritic shaft just below the spine (broken curve) as a function of relative timing between the two conductance changes. Both input functions of the form of figure 4 have $t_{peak} = 0.25$ ms with $g_{e\,max} = 10^{-8}$ S and $g_{i\,max} = 10^{-7}$ S. The corresponding voltage is the full solution of the coupled Volterra equations (19). The halfwidth of the curves is 0.12 and 0.22 ms for the spine and the dendrite case respectively.

FIGURE 8. Nonlinear addition as a function of synaptic input amplitude for three different situations. For the three pairs of curves, the upper continuous curve is $V_{s1} + V_{s2}$, i.e. the sum of the individual evoked somatic potentials, while the lower dotted curve represents V_{s1+2}, i.e. the somatic potential generated while both synapses are simultaneously active (the two curves overlap in the third case). The driving potential (80 mV) and the steady-state synaptic inputs g_1 are the same for both synapses. For the top pair of curves both synapses lie directly on the apical tree, for the middle pair of curves both are situated on two standard spines ($l_n = 1.0$ μm and $d_n = 0.1$ μm) and for the bottom curve both are on elongated spines ($l_N = 2.0$ μm and $d_N = 0.05$ μm). The spines are 26 μm apart (0.05 times the electrotonic distance) and are located in the middle part of the apical tree.

7.2. *Nonlinear addition*

We now determine the degree of nonlinear addition between two excitatory synapses lying close together, with the same driving potential E and the same steady-state conductance input g. We are specifically interested in the summation of potential for two synapses lying on nearby spines. The effect of nonlinear addition can be appreciated best when the sum of the somatic potential generated when both synapses are active alone $V_{s1} + V_{s2}$ is compared with the somatic depolarization when both fire simultaneously (V_{s1+2}; see equation (19)). In figure 8 we have plotted both voltages as a function of the strength of the steady-state synaptic input for three different situations. The upper pair of curves show $V_{s1} + V_{s2}$

and V_{s1+2} for the case when both synapses lie on the apical tree 26 μm apart; the middle pair of curves are for synapses lying on two standard spines ($l_N = 1.0$ μm and $d_N = 0.1$ μm) and the bottom curve (where the two voltage functions overlap) is for two stretched spines ($l_N = 2.0$ μm and $d_N = 0.05$ μm). In the last case there is practically no nonlinear addition since $V_{s1} + V_{s2}$ and V_{s1+2} differ only by a very slight amount. This is associated, however, with a very strong nonlinear saturation within one spine. The other extreme is represented by the situation where both synapses lie on the apical tree. For large inputs the potential is saturated; i.e. adding a second synapse does not change the somatic depolarization appreciably. Thus there is a trade-off between nonlinear addition of the synapses and saturation within the postsynaptic site. Once again, when synaptic inputs are small, they can be considered as currents and nonlinear effects do not occur.

8. Do these results depend on parameter values?

We stress that the quantitative values computed for our pyramidal cell depend on the parameter values assumed. While our calculations are based on commonly observed values for cortical cells, the reasonable physiological range is relatively wide.

For pyramidal cells in the hippocampus, larger membrane time constants are reported than used here (Brown *et al.* 1981*a*; Johnston 1981). This would imply a value of R_m about two to three times as large as we have assumed, while, for motoneurons of the cat, membrane resistance values range between 1000 and 2000 Ω cm^2 (Barrett & Crill 1974; Barrett 1975). Figure 3*a* shows the variation of the spine input resistance K_{11} as a function of the neck geometry for different R_m values (1000, 4000 and 16000 Ω cm^2). As expected from (16) the resulting change in K_{11} is slight since the spine neck resistance R_N is independent of R_m to a very good approximation. Thus, apart from an increase in the effect of a changing spine geometry on somatic depolarization, our basic results are still valid.

Values for the membrane capacity C_m much different from the one that we have used are not very likely (Brown *et al.* 1981*b*); in any case C_m does not affect our steady state values.

The resistivity of the cytoplasm is rather constant at about 70 Ω cm for several vertebrate neurons (Barrett & Crill 1974; Rall 1977). It seems unlikely that R_i is lower than 50 Ω cm (Barrett 1975). Within this range of values our results would not be drastically affected. However, owing to the presence, at least in mammalian cerebral cortex, of the spine apparatus and related organelles in many spines (Gray 1959; Peters & Kaiserman-Abramof 1970), the specific resistivity of the spines could be significantly higher than the resistivity of the dendrites and the soma. Figure 3*a* (dot–dashed curve) shows K_{11} for such a case. The specific resistivity of the soma and the dendrites was assumed to be 70 Ω cm while the R_i value of the spine (neck and head) was doubled to 140 Ω cm; since K_{11} depends linearly on R_i there is a significant increase in spine input resistance. This would cause a much stronger nonlinear behaviour than with a homogeneous value of R_i, without leading to an increase in the maximal evoked somatic potential.

All of our conclusions rest on the assumption of passive or non-regenerative

membrane properties. The situation could change if the dendrite or even the spine itself were capable of producing spikes or if voltage-dependent channels were activated. A systematic under- or overestimation of the diameter of dendrites could influence strongly our conclusions. If the dendritic processes were much finer than we measured, the input impedances $K_{ii}(\omega)$ would be very high throughout the dendritic tree; a synapse on a dendrite would then be much more similar to a synapse on a spine.

Precise data about conductance changes at a spine and their time course seem much more difficult to obtain. As all our data make abundantly clear, the size of the conductance change is critical for determining the operating range of the spine and its actual properties (see Discussion).

9. Discussion

A main point of our investigation is reflected in figures 2 and 5. If we assume that there is only a single excitatory input, spines show significant nonlinear saturation. Even for very fast conductance changes, the effect of the spine is to map a possible wide range of input amplitudes (g_1) onto a restricted set of output values (V_s) or, in other words, to perform nonlinear range compression (figure 2). In spines the saturation effect becomes especially characteristic for transient inputs, since a short input can induce much higher depolarization in the spine than in the dendrite. As Perkel has suggested (D. H. Perkel & T. H. Brown, personal communication), this large depolarization may have functional significance in conjunction with possible active membrane properties of the spine. Saturation goes hand in hand with reduced nonlinear addition between synapses situated on different spines, resulting in a more linear behaviour between simultaneously active synapses (figure 8). This might explain the results of Andersen & Langmoen (1981) who found that simulating nearby synapses (situated on spines) in the dendritic tree of CA1 pyramidal cells results in a linear summation of the corresponding e.p.s.ps.

Saturation itself does not make the spine so interesting, since the dendrite also exhibits nonlinear saturation, albeit to a much lesser extent. What is important is that the spine can effectively control the attenuation of its input via the dimensions of the neck, setting the shape of the gain control curve (figures 3*b*, 6). Optimal control takes place in the intermediate range, i.e. for $0.1 < g_1 K_{11} < 10.0$. Stretching the spine neck from 1.0 to 14 μm in length can reduce the somatic potential for fast transients from 0.26 to 0.11 mV (−58 %), while shortening the neck to 0.6 μm increases the depolarization to 0.54 mV (+108 %; Koch 1982). The differences in spine neck length observed experimentally within one cell can be much larger (Peters & Kaiserman-Abramof 1970).

An important conclusion of our analysis is that a small change in spine dimensions around the optimal value can produce a large change in the 'weight' of the synapse. Since spines are so numerous that the total effect on the somatic potential can be biophysically quite effective. According to our calculations, the magnitude of the structural change to be expected is small for individual spines, making their observation by present morphological methods very difficult. Changes

of the dimensions of all the spines on a neuron may be observable in special cases, as for instance in the experiment by Boycott (1982).

This facilitation effect can be further augmented either by increasing the membrane resistance or by increasing the specific resistivity of the cytoplasm within the spine. The advantage of the latter proposal is the fact that this would increase the nonlinearity while lowering the evoked somatic potential, leading to a higher number of synapses that must be active to elicit a spike. If the input is too small ($g_1 K_{11} < 0.1$) the spine is working in the linear range, where conductance inputs can be considered as current inputs and the somatic potential does not depend any more on the spine itself, but only on the position of the spine relative to the soma (K_{1s}). If the input is too large ($g_1 K_{11} > 10.0$) the spine is saturated and the somatic potential is independent of the strength of the synaptic input. Since, at least for cortical pyramidal cells, spiny cells require the simultaneous activation of a few hundred excitatory inputs to produce a spike (for estimates in hippocampus cells see Andersen & Langmoen (1981) or McNaughton *et al.* (1981); see also Braitenberg (1981)), nonlinear saturation at large input values could be a mechanism used by the central nervous system for preventing any one input from dominating over the other inputs.

The same mechanism could also explain the well known fact that the soma and the first 20–30 μm of the primary dendrites are practically devoid of spines (cf.: White & Rock 1980; Parnavelas *et al.* 1977; Wilson & Groves 1980). Proximal or somatic spines could, already at rather small inputs (see figure 2*a*), dominate the firing pattern of the cell, masking completely the effect of more distal spines. Perhaps to prevent this, natural selection has ensured the absence of any spines on or near the soma; when exceptions are found (see Scheibel & Scheibel 1968) the total somatic spine population is very small and their appearance is long, slim and with a tiny head, thus maximizing input resistance (figure 2*a*, bottom curve).

It has repeatedly been reported (Berard *et al.* 1981; Laatch & Cowan 1966; Jones & Powell 1969; Coss & Globus 1978) that long thin spines are more frequent at distal dendritic locations while near the cell body and around the base of the primary dendrite more short, stubby spines predominate. This would seem to handicap distal spines twice over: the attenuation from distal locations to the soma is enhanced by increasing the spine input resistance of the distal spines. In the light of the experimental fact that distal synapses are often equally as effective in eliciting somatic spikes as are proximal synapses (Andersen *et al.* 1980; Redman & Walmsley 1981; Iansek & Redman 1973), one would expect the opposite effect, distal spines compensating for their disadvantage by lowering their input impedance while proximal spines compensate for their preferential position by increased spine input resistance. To that end distal spines should be short and stubby and proximal spines long and thin. This however has never been observed. Rall (1974) postulated that the increase in spine input resistance with increasing distance from the cell soma maximizes the gain control property of spines, small variations in neck dimensions leading to large changes in potential. He proposed that the optimal range of the spine neck occurs when the neck resistance R_N is approximately matched by the input impedance K_{22} of the dendrite. His argument is strictly correct

only for large g_1 values, when equation (18) reduces to $R_N \approx K_{22}$. In the general case the 'optimal operating range' depends on location and on strength of the input. In table 2 we have determined for different steady-state synaptic inputs the corresponding dimensions of the spine neck for the proximal, the middle and the distal spine of figure 1. For small conductance changes the spines work in the linear range and the difference in geometry of the necks is too small to be of any

TABLE 2. SPINE NECK DIMENSIONS FOR OPTIMAL PLASTICITY DETERMINED FROM EQUATIONS (16) AND (18) FOR DIFFERENT STEADY-STATE CONDUCTANCE CHANGES AND LOCATIONS (SEE ARROWS IN FIGURE 1)

(The upper value gives the spine neck length $l_N/\mu m$ and the lower value the neck diameter $d_N/\mu m$. The total spine neck area $d_N\, l_N$ is always constant at 0.1 μm^2.)

	proximal spine	middle spine	distal spine
K_{22} ...	25.74	53.38	109.26
$g_1/\mu S$			
10^{-3}	1.792	1.808	1.839
	0.056	0.055	0.054
10^{-2}	0.890	0.951	1.055
	0.112	0.105	0.095
10^{-1}	0.585	0.708	0.875
	0.171	0.141	0.114

relevance. For larger inputs (10^{-7} S) the changes in optimal dimensions increase considerably (there is a 50% length increase and 33% diameter decrease from proximal to distal). This is of the same order of magnitude as measured experimentally (Coss & Globus 1978). Thus our exact calculations confirm Rall's earlier hypothesis that the observed dependence of spine dimensions on their locations could be ascribed to the fact that this changing shape implies optimal control.

As suggested by B. B. Boycott (personal communication), some caution is needed here: the diversity of spine shapes on a single cell could also be related to different types of inputs. Furthermore, the dependence of spine length on location may have simple explanations, for instance in terms of a different growth rate at distal and proximal locations.

Although the correlation between structure and function of synapses is not yet conclusively established, there is growing evidence associating Gray type 1 (asymmetrical) synapses with excitatory synapses and Gray type 2 (symmetrical) synapses with inhibitory synapses (Peters *et al.* 1970). Based on these morphological criteria it is found that most spines carry an excitatory synapse. This makes a lot of sense when one considers the nonlinear interaction between synapses of opposing sign (table 1). If we assume that the inhibitory reversal potential is not too far away from the membrane resting potential, a single inhibitory synapse on a spine is not very effective in reducing the potential due to an excitatory input somewhere else. Moving an inhibitory synapse from the direct path (in this case the apical dendrite) onto a nearby spine can reduce the F-factor by as much as 50%. In

agreement with these calculations, inhibitory synapses are almost always found either on the dendritic shaft or on the soma (Parnavelas *et al.* 1977; Wilson & Groves 1980; White & Rock 1980)†.

A significant exception to this rule are spines that carry both symmetrical and asymmetrical synapses on them (White & Rock 1980; Jones & Powell 1969; Scheibel & Scheibel 1968; Peters & Kaiserman-Abramof 1969, 1970; Sloper & Powell 1979). Quite apart from the interesting possibility of synthesizing local circuits by a variety of different computations (for an example of a multiplication-like operation see Torre & Poggio (1978) and Poggio & Torre (1981); see also Scheibel & Scheibel (1968)), the conjunction of excitatory and inhibitory synapses on a single spine seems to offer the possibility of constructing a time-discrimination circuit with a temporal resolution of the order of 100 μs, for input pulses lasting somewhat under 1 ms. Using a spine with an excitatory and a shunting inhibitory synapse and working with inputs lasting about 1 ms, we find that delaying inhibition by just 0.1 ms with respect to the start of excitation makes this inhibition practically inefficient in reducing the somatic depolarization due to the excitation. Using inputs $g_e(t)$ and $g_i(t)$ with an equal short rise time but a more slowly decaying phase, the 'tuning curve' of figure 7 would become much more asymmetric, with the F-factor for negative delays being rather high but dropping very quickly to 1.0 for positive delays (by positive delay we mean inhibition after excitation). Inhibitory conductance changes seem indeed to last much longer than excitatory conductance changes in the cases analysed so far. Such a mechanism might possibly be used in the neuronal circuit responsible for the startle response in teleost fish (Diamond *et al.* 1970; Celio *et al.* 1979). Thus, spines with both excitatory and inhibitory synapses on them could well represent locations where the interactions between two individual inputs could be very specific, both in time and in space.

10. Functional considerations

So, finally, what could be the functions of spines? Since in this study we have only considered the electrophysiological aspects of spines, we exclude from our discussion suggestions such as those of Peter & Kaiserman-Abramof (1970) or Swindale (1981) on the uses of spines to connect axons and dendrites via *en passant* synapses on spines. Three different possibilities could be envisaged, none excluding the others.

First of all, spines compress the range of each single excitatory synapse, mapping a wide range of inputs onto a limited range of outputs. Spines show a high sensitivity to small inputs and keep the maximum depolarization that can be achieved by a single synapse below a certain value (dependent on the spine and its position relative to the soma). Furthermore, they tend to isolate individual synapses on spines from the depolarization generated by simultaneously active synapses elsewhere. It is important that this saturation property holds also for very fast inputs, in sharp contrast with the case of a synapse on a dendrite or the soma.

† There are a few exceptions to this rule: see Kosaka (1980) or Peters & Kaiserman-Abramof (1970), who find spines on the soma or on the initial segment with symmetrical synaptic profiles.

Secondly, a fine control of synaptic efficiency via the spine diameter (and/or length) may represent a basic mechanism for learning. This requires a conductance change outside the linear range, implying that spines that do not fulfil this condition have no interesting electrical function. Repeated activation of a synapse on a spine could enlarge spine dimensions by some mechanism and thereby enhance synaptic potency.

This postsynaptic mechanism may underly long-term potentiation in the pyramidal cells of the hippocampus (see Introduction) and the changes in cortical functional connectivity taking place during early visual exposure (Rauschecker & Singer 1981; Schüz 1981). Spine plasticity could also play the decisive role during learning in the cerebellum. This suggestion is based on the general framework of neuronal plasticity in the cerebellum as laid down by Marr (1969) and later modified by Albus (1971). Marr proposed the following: the main cerebellar input, the mossy fibres, which excite the only output of the cerebellum, the Purkinje cells, polysynaptically through the granular cells and their axons (the parallel fibres) can be reorganized by the simultaneous activation of the second cerebellar input, the climbing fibres, which make very powerful synapses onto the Purkinje cells. Specifically, his hypothesis requires that the conjunction of an active parallel fibre and an active climbing fibre raises the transmission of the parallel fibre–Purkinje cell synapse, which is always on a spine. Albus (1971) later posulated instead of a synaptic facilitation a synaptic depression which seems to agree better with present experimental data (Llinás 1981; Ito *et al.* 1982; Andersen 1982). This effect could very well be due to a change in spine neck dimensions, induced perhaps by change in membrane potential (Stent 1973). Contractile proteins have been suggested as the mechanism underlying the change in shape of spines (Crick 1982). Recently, Fifkova & Delay (1982) and Matus *et al.* (1982) have shown that actin is indeed present at high concentrations in dendritic spines. Thus the modification of spine shape could be one of the mechanisms responsible for learning and memory in the central nervous system.

Thirdly, the conjunction of an excitatory and inhibitory synapse on the same spine could represent a circuit responsible for various very selective computations, such as multiplication or time discrimination with a temporal resolution well below the millisecond range (Diamond *et al.* 1970).

We are grateful to B. B. Boycott, F.R.S., V. Braitenberg, F. H. C. Crick, F.R.S., K. Hausen, K. Nielsen and J. Rauschecker for reading various versions of the manuscript and for many comments and ideas. A. Schüz, F. H. C. Crick, V. Braitenberg and V. Torre aroused our interest in the properties of spines. We are also indebted to V. Braitenberg, who kindly provided the histological material on which our analysis is based. T. Wiegand helped us with the figures. This work was done at the Max Planck Institut für biologische Kybernetik. C. K. was supported by a fellowship from the Studienstiftung des deutschen Volkes and is presently supported by the Fritz Thyssen Stiftung. Support for T.P. is provided by the Advanced Research Projects Agency of the Department of Defense under Office of Naval Research contract N00014-75-C-0643 and by the National Science Foundation grant MCS-79-23110. Travel for collaboration purposes was supported under N.A.T.O. grant number 237.81.

References

Albus, J. S. 1971 A theory of cerebellar function. *Mathl Biosci.* **10**, 25–61.

Andersen, P. 1982 Cerebellar synaptic plasticity – putting theories to the test. *Trends Neurosci.* **5**, 324–325.

Andersen, P. & Langmoen, I. A. 1981 Synaptic interaction on hippocampal pyramids. In *28th International congress of physiological sciences* (ed. E. Grastyan & P. Molnar), pp. 269–273. Budapest: Akadémiai Kiadó.

Andersen, P., Silfvenius, H., Sundberg, S. H. & Sveen, O. 1980 A comparison of distal and proximal dendritic synapses on CA1 pyramids in guinea-pig hippocampal slices *in vitro*. *J. Physiol., Lond.* **307**, 273–299.

Barrett, J. N. 1975 Motoneuron dendrites: role in synaptic integration. *Fedn Proc. Fedn Am. Socs exp. Biol.* **34**, 1398–1407.

Barrett, J. N. & Crill, W. E. 1974 Specific membrane properties of cat motoneurons. *J. Physiol., Lond.* **239**, 301–324.

Berard, D. R., Burgess, J. W. & Coss, R. G. 1981 Plasticity of dendritic spine formations: a state dependent stochastic process. *Int. J. Neurosci.* **13**, 93–98.

Bliss, T. V. & Lømo, T. 1973 Long-lasting potentiation of synaptic transmission in the dentate area of the anaesthetized rabbit following stimulation of the perforant path. *J. Physiol., Lond.* **232**, 331–356.

Boycott, B. B. 1982 Experiments on dendritic spines. *Trends Neurosci.* **5**, 328–329.

Bradley, P. & Horn, G. 1979 Neuronal plasticity in the chick brain: morphological effects of visual experience on neurons in hyperstriatum accessorium. *Brain Res.* **162**, 148–153.

Braitenberg, V. 1981 A selection of facts and conjectures about the cerebral cortex inspired by the theory of cell assemblies. In *28th International congress on physiological sciences* (ed. Gy. Szekely, E. Labos & S. Damjanovich), pp. 287–289. Budapest: Akadémiai Kiadó.

Brandon, J. G. & Coss, R. G. 1982 Rapid dendritic spine stem shortening during one-trial learning: the honeybee's first orientation flight. *Brain Res.* **252**, 51–61.

Brown, T. H., Fricke, R. A. & Perkel, D. H. 1981*a* Passive electrical constants in three classes of hippocampal neurons. *J. Neurophysiol.* **46**, 812–827.

Brown, T. H., Perkel, D. H., Norris, J. C. & Peacock, J. H. 1981*b* Electronic structure and specific membrane properties of mouse dorsal root ganglion neurons. *J. Neurophysiol.* **45**, 1–15.

Butz, E. G. & Cowan, J. D. 1974 Transient potentials in dendritic systems of arbitrary geometry. *Biophys. J.* **14**, 661–689.

Celio, M. R., Gray, E. G. & Yasargil, G. M. 1979 Ultrastructure of the Mauthner axon collateral and its synapses in the goldfish spinal cord. *J. Neurocytol.* **18**, 19–29.

Chang, H. T. 1952 Cortical neurons with particular reference to the apical dendrites. *Cold Spring Harb. Symp. quant. Biol.* **17**, 189–202.

Coss, R. G., Brandon, J. G. & Globus, A. 1980 Changes in morphology of dendritic spines on honeybee calycal interneurons associated with cumulative nursing and foraging experiences. *Brain Res.* **192**, 49–59.

Coss, R. G. & Globus, A. 1978 Spine stems on tectal interneurons in jewel fish are shortened by social stimulation. *Science, N.Y.* **200**, 787–789.

Creutzfeldt, O. D., Lux, H. D. & Nacimiento, A. C. 1964 Intracelluläre Reizung corticaler Nervenzellen. *Pflügers Arch. ges. Physiol.* **281**, 120–151.

Crick, F. 1982 Do dendritic spines twitch? *Trends Neurosci.* **5**, 44–46.

Diamond, J., Gray, E. G. & Yasargil, G. M. 1970 The function of the dendritic spine: a hypothesis. In *Excitatory synaptic mechanisms* (ed. P. Andersen & J. Jansen), pp. 212–222. Oslo Universitetsforlag.

Eccles, J. C. 1979 Synaptic plasticity. *Naturwissenschaften* **66**, 147–153.

Fifkova, E. & Anderson, C. L. 1981 Stimulation-induced changes in dimensions of stalks of dendritic spines in the dentate molecular layer. *Expl Neurol.* **74**, 621–627.

Fifkova, E., Anderson, C. L., Young, S. J. & Van Harreveld, A. 1982 Effect of anisomycin on stimulation-induced changes in dendritic spines of the dentate granule cells. *J. Neurocytol.* **11**, 183–210.

Fifkova, E. & Delay, R. 1982 Cytoplasmic actin in neuronal processes as a possible mediator of synaptic plasticity. *J. Cell Biol.* **95**, 345–350.

Fifkova, E. & Van Harreveld, A. 1977 Long-lasting morphological changes in dendritic spines of dentate granular cells following stimulation of the entorhinal area. *J. Neurocytol.* **6**, 211–230.

Gray, E. G. 1959 Axo-somatic and axo-dendritic synapses of the cerebral cortex: an electron microscope study. *J. Anat.* **93**, 420–433.

Iansek, R. & Redman, S. J. 1973 The amplitude, time course and charge of unitary excitatory post-synaptic potentials evoked in spinal motoneurone dendrites. *J. Physiol., Lond.* **234**, 665–688.

Ito, M., Masaki, S. & Tongrooch, P. 1982 Climbing fibre induced depression of both mossy fibre responsiveness and glutamate sensitivity of cerebellar Purkinje cells. *J. Physiol., Lond.* **324**, 113–134.

Jack, J. J., Noble, D. & Tsien, R. W. 1975 *Electric current flow in excitable cells.* Oxford: Clarendon Press.

Johnston, D. 1981 Passive cable properties of hippocampal CA3 pyramidal neurons. *Cell. molec. Neurobiol.* **1**, 41–55.

Jones, E. G. & Powell, T. P. S. 1969 Morphological variations in the dendritic spines of the neocortex. *J. Cell Sci.* **5**, 509–529.

Koch, C. 1982 Nonlinear information processing in dendritic trees of arbitrary geometries. Ph.D. thesis, University of Tübingen.

Koch, C. & Poggio, T. 1983 Electrical properties of dendritic spines. *Trends Neurosci.* **6**, 80–83.

Koch, C., Poggio, T. & Torre, V. 1982 Retinal ganglion cells: a functional interpretation of dendritic morphology. *Phil. Trans. R. Soc. Lond.* B **298**, 227–264.

Koch, C., Poggio, T. & Torre, V. 1983 Nonlinear interaction in a dendritic tree: localization, timing and role in information processing. *Proc. natn. Acad. Sci. U.S.A.* (In the press.)

Kosaka, T. 1980 The axon initial segment as a synaptic site: ultrastructure and synaptology of the initial segment of the pyramidal cell in the rat hippocampus (CA3 region). *J. Neurocytol.* **9**, 861–882.

Laatch, R. H. & Cowan, W. M. 1966 Electron microscopic studies of the dentate gyrus of the rat. I. Normal structure with special reference to synaptic organization. *J. comp. Neurol.* **128**, 359–396.

Llinás, R. R. 1981 Cerebellar modeling. *Nature, Lond.* **291**, 279–280.

Marin-Padilla, M. 1974 Structural organization of the cerebral cortex (motor area) in human chromosomal aberration. A golgi study: I. D_1 (13–15) Trisomy, Patau Syndrome. *Brain Res.* **66**, 375–391.

Marr, D. 1969 A theory of cerebellar cortex. *J. Physiol., Lond.* **202**, 437–470.

Matus, A., Ackermann, M., Pehling, G., Byers, H. R. & Fujiwara, K. 1982 High actin concentrations in brain dendritic spines and postsynaptic densities. *Proc. natn. Acad. Sci. U.S.A.* **79**, 7590–7594.

McNaughton, B. L., Barnes, C. A. & Andersen, P. 1981 Synaptic efficacy and EPSP summation in granule cells of rat fascia dentata studied *in vitro*. *J. Neurophysiol.* **46**, 952–966.

Parnavelas, J. G., Sullivan, K., Lieberman, A. R. & Webster, K. E. 1977 Neurons and their synaptic organization in the visual cortex of the rat. *Cell Tiss. Res.* **183**, 499–517.

Peters, A. & Kaiserman-Abramof, I. R. 1969 The small pyramidal neuron of the cerebral cortex *Z. Zellforsch. mikrosk. Anat.* **100**, 487–506.

Peters, A. & Kaiserman-Abramof, I. R. 1970 The small pyramidal neuron of the rat cerebral cortex. The perikaryon, dendrites and spines. *Am. J. Anat.* **127**, 321–356.

Peters, A., Palay, S. L. & Webster, H. de F. 1970 *The fine structure of the nervous system.* Philadelphia: Saunders.

Poggio, T. & Torre, V. 1981 A theory of synaptic interaction. In *Theoretical approaches in neurobiology* (ed. W. Reichardt & T. Poggio), pp. 28–38. Cambridge, Massachusetts: M.I.T. Press.

Purpura, D. 1974 Dendritic spines 'dysgenesis' and mental retardation. *Science, N.Y.* **186**, 1126–1128.

Purpura, D. 1979 Pathobiology of cortical neurons in metabolic and unclassified amentias. In *Congenital and acquired cognitive disorders* (ed. R. Katzman), pp. 43–68. New York: Raven Press.

Rall, W. 1970 Cable properties of dendrites and effects of synaptic location. In *Excitatory synaptic mechanisms* (ed. P. Andersen & J. Jansen), pp. 175–187. Oslo Universitetsforlag.

Rall, W. 1974 Dendritic spines, synaptic potency and neuronal plasticity. In Cellular mechanisms subserving changes in neuronal activity (ed. C. D. Woddy, K. A. Brown, T. J. Crow & J. D. Knispel). *Brain Inf. Serv. Res. Rep.* **3**, 13–21.

Rall, W. 1977 Core conductor theory and cable properties of neurons. In *Handbook of physiology* (ed. E. Kandel & S. Geiger), vol. 1, pp. 39–97. Washington, D.C.: American Physiological Society.

Rall, W. 1978 Dendritic spines and synaptic potency. In *Studies in Neurophysiology* (ed. R. Porter), pp. 203–209. Cambridge University Press.

Rausch, G. & Scheich, H. 1982 Dendritic spine loss and enlargement during maturation of the speech control system in the mynah bird (*Gracula religiosa*). *Neurosci. Lett.* **29**, 129–133.

Rauschecker, J. P. & Singer, W. 1981 The effects of early visual experience on the cats visual cortex and their possible explanation by Hebb synapses. *J. Physiol., Lond.* **310**, 215–239.

Redman, S. & Walmsley, B. 1981 The synaptic basis of the monosynaptic stretch reflex. *Trends Neurosci.* **4**, 248–250.

Scheibel, M. E. & Scheibel, A. B. 1968 On the nature of dendritic spines. Report of a workshop. *Commun. behav. Biol.* A **1**, 231–265.

Schüz, A. 1976 Pyramidal cells with different densities of dendritic spines in the cortex of the mouse. *Z. Naturf.* **31** c, 319–326.

Schüz, A. 1981 Pränatale Reifung und postnatale Veränderung im Cortex des Meerschweinchens: Mikroskopische Auswertung eines natürlichen Deprivationsexperimentes. II. Postnatale Veränderungen. *J. Hirnforsch.* **22**, 113–127.

Sloper, J. J. & Powell, T. P. S. 1979 An experimental electron microscopic study of afferent connections to the primate motor and somatic sensory cortices. *Phil. Trans. R. Soc. Lond.* B **285**, 199–226.

Stent, G. S. 1973 A physiological mechanism for Hebb's postulate of learning. *Proc. natn. Acad. Sci. U.S.A.* **70**, 997–1001.

Swanson, L. W., Teyler, T. J. & Thompson, R. F. 1982 Hippocampal long-term potentiation: mechanisms and implications for memory. *Neurosci. Res. Prog. Bull.* **20**, 613–769.

Swindale, N. V. 1981 Dendritic spines only connect. *Trends Neurosci.* **4**, 240–241.

Torre, V. & Poggio, T. 1978 A synaptic mechanism possibly underlying directional selectivity to motion. *Proc. R. Soc. Lond.* B **202**, 409–416.

Valverde, F. 1967 Apical dendritic spines of the visual cortex and light deprivation in the mouse. *Expl Brain Res.* **3**, 337–352.

Van Harreveld, A. & Fifkova, E. 1975 Swelling of dendritic spines in the fascia dentata after stimulation of the perforant fibers as a mechanism of post-tetanic potentiation. *Expl Neurol.* **49**, 736–749.

Westrum, L. E. & Blackstad, T. W. 1982 An electron microscopic study of the stratum radiatum of the rat hippocampus with particular emphasis on synaptology. *J. comp. Neurol.* **119**, 281–309.

White, E. L. & Rock, M. P. 1980 Three-dimensional aspects and synaptic relationships of a Golgi-impregnated spiny stellate cell reconstructed from serial thin sections. *J. Neurocytol.* **9**, 615–636.

Wilson, C. J. & Groves, P. M. 1980 Fine structure and synaptic connections of the common spiny neuron of the rat neostriatum: a study employing intracellular injection of horseradish perioxidase. *J. comp. Neurol.* **194**, 599–615.